Available online at www.sciencedirect.com

ScienceDirect

Mendeleev Commun., 2023, **33**, 553–555

Mendeleev Communications

Ionically cross-linked micro-sized hydrogels with encapsulated drug: structure, cell uptake kinetics and cytotoxicity

Vasily V. Spiridonov,*[a] Alina R. Lukmanova,[b] Denis V. Pozdyshev,[c] Alina A. Markova,[d] Yuliya L. Volodina,[e] Galina V. Golovina,[d] Vladimir V. Shakhmatov,[d] Vladimir A. Kuzmin,[d] Vladimir I. Muronetz[c] and Alexander A. Yaroslavov[a]

[a] *Department of Chemistry, M. V. Lomonosov Moscow State University, 119991 Moscow, Russian Federation. E-mail: vasya_spiridonov@mail.ru*
[b] *Department of Materials Science, M. V. Lomonosov Moscow State University, 119991 Moscow, Russian Federation*
[c] *A. N. Belozersky Research Institute of Physico-Chemical Biology, M. V. Lomonosov Moscow State University, 119992 Moscow, Russian Federation*
[d] *N. M. Emanuel Institute of Biochemical Physics, Russian Academy of Sciences, 119334 Moscow, Russian Federation*
[e] *N. N. Blokhin National Medical Research Center of Oncology, 115478 Moscow, Russian Federation*

DOI: 10.1016/j.mencom.2023.06.036

Micro-sized hydrogels synthesized by electrostatic cross-linking of anionic alginate with Ca^{2+} cations were additionally loaded with cationic fluorescent dye Rhodamine 6B or cationic antitumor antibiotic doxorubicin. Forming complexes with Ca^{2+} alginate hydrogels, doxorubicin retained or even reduced its toxicity to tumor and normal cells. The results can be used to design containers for the encapsulation and delivery of drugs and control their interaction with cells.

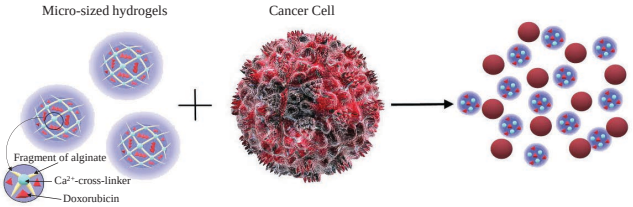

Keywords: sodium alginate, cross-linked hydrogels, rhodamine, doxorubicin, intracell migration, cytotoxicity.

Immobilization of a drug on the surface of micro-sized particles or incorporation of a drug inside particles makes it possible to concentrate hundreds and thousands of bioactive molecules in a small volume, protect the molecules from an aggressive environment and increase the circulation time of the drug in the body.[1] With this technique, the maximum therapeutic effect of the drug is achieved with minimal side effects.[2] Among polymeric drug carriers, water-soluble polyethylene oxides, polypropylene oxides, polyvinyl alcohol and polylactides, as well as lipid-based nanoparticle carriers, are often used.[3–6] Anionic polymers (polyanions) are of particular interest because of their ability to electrostatically bind various cationic bioactive substances.[7–9] The polyvalent cations act as cross-linking agents, causing the collapse of anionic macromolecules and the formation of nano-sized ionically cross-linked hydrogels.[10]

Anionic polysaccharides of natural origin, *e.g.*, sodium salts of alginic acid and carboxymethylcellulose, degrade down to small fragments by the action of enzymes.[11] This makes polysaccharides promising carriers for drug encapsulation and release.[12] After drug delivery is complete, the polysaccharide carrier can be digested by enzymes[13] and excreted from the body.

In this article, we describe the synthesis of nano-sized alginate hydrogels cross-linked with Ca^{2+} ions, the loading of these hydrogels with a fluorescent rhodamine dye, the kinetics of penetration of the rhodamine-containing hydrogel through the cell membrane, the preparation of the Ca^{2+} alginate hydrogels containing the encapsulated antitumor antibiotic doxorubicin (Dox) and the cytotoxicity of the Dox-loaded hydrogels. Taken together, these results reflect the interrelated properties of hydrogel dosage forms: their composition, transport through the biological membrane and biological activity.

To prepare Ca^{2+} alginate hydrogels, an aqueous solution of sodium alginate (Sigma–Aldrich, analytical grade) was added dropwise simultaneously with various aliquots of an aqueous solution of calcium chloride (Sigma–Aldrich, analytical grade) with the vigorous stirring. As a result, a series of hydrogels HG-1, HG-2 and HG-3 were obtained with the molar ratio of anionic alginate units (ALGs) and Ca^{2+} cations, Z_{Ca} = [ALG]/[Ca^{2+}], equal to 15, 10 and 7, respectively. Each hydrogel contained an excess of anionic ALGs, which provided a total negative charge to hydrogel particles and their resistance to aggregation in aqueous solutions. The electrophoretic mobility of hydrogel particles (a parameter related to their surface charge) is presented in Table 1,

Table 1 Electrophoretic mobility (EPM), hydrodynamic diameter (D) and molecular weight (M_w) of the initial sodium alginate and the resulting Ca^{2+} alginate hydrogels.[a]

Sample	EPM/m^2 V^{-1} s^{-1}	D/nm	M_w/kDa
Na alginate	$-(3.75 \pm 0.07) \times 10^{-8}$	680 ± 19	$(2.7 \pm 0.4) \times 10^3$
HG-1	$-(3.41 \pm 0.07) \times 10^{-8}$	405 ± 17	$(5.8 \pm 0.4) \times 10^3$
HG-2	$-(2.10 \pm 0.05) \times 10^{-8}$	270 ± 14	$(36 \pm 1) \times 10^3$
HG-3	$-(1.95 \pm 0.04) \times 10^{-8}$	210 ± 11	$(42 \pm 3) \times 10^3$

[a] Hydrodynamic and electrokinetic measurements were performed using a Brookhaven Instruments particle analyzer.

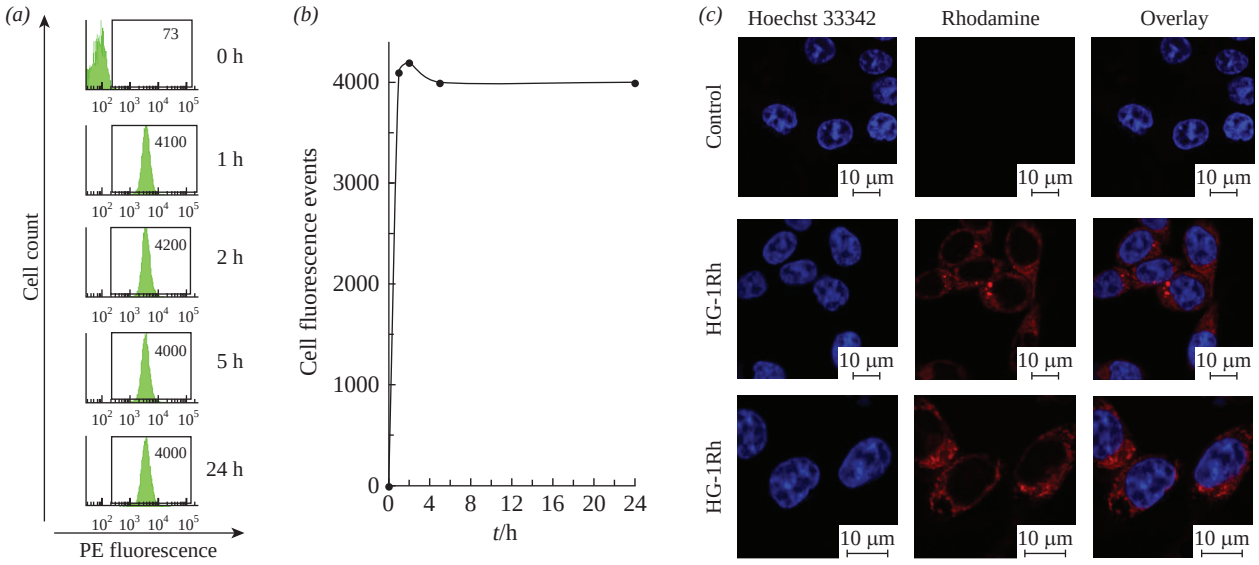

Figure 1 (*a*) Flow cytometry analysis of HCT116 cells incubated with HG-1Rh for various times. (*b*) Kinetics of HG-1Rh penetration into HCT116 cells. (*c*) Confocal microscopy images of HCT116 cells with HG-1Rh inside (see text for details).

which also shows data on the hydrodynamic diameter and molecular weight of the hydrogels, measured using dynamic and static light scattering, respectively. Table 1 also shows the corresponding data for the initial sodium alginate.

Three conclusions follow from the data in Table 1. Firstly, the electrostatic complexation of Ca^{2+} cations with alginate leads to gradual neutralization of the negative charge of alginate and a decrease in the absolute value of the EPM from 3.75×10^{-8} m^2 V^{-1} s^{-1} for the initial alginate to 1.95×10^{-8} m^2 V^{-1} s^{-1} for the HG-3 hydrogel with the maximum content of Ca^{2+} cations. Secondly, the complexation is accompanied by the collapse of the alginate matrix, which is expressed in a decrease in the hydrodynamic diameter from 680 nm for the initial alginate to 210 nm for the HG-3 hydrogel. These conclusions agree well with the results of other studies on the electrostatic interaction of ions with polymers.[14]

The third conclusion concerns the molecular weights of hydrogels complexed with Ca^{2+} cations. Assuming the molecular weight of the ALG unit with one carboxyl group (M_{ALG}) is 216 Da[15] and the molecular weight of the Ca^{2+} ion (M_{Ca}) is 40 Da, and the fact that each Ca^{2+} ion forms ionic bonds with two anionic ALG groups, one can calculate the molecular weight of the ALG unit complexed with Ca^{2+} cations ($M_{Ca–ALG}$) as

$$M_{Ca–ALG} = M_{ALG} + M_{Ca}/2Z_{Ca}, \quad (1)$$

and then the molecular weight of Ca^{2+} alginate hydrogel as

$$M_{w(calc)} = (M_{Ca–ALG}/M_{ALG}) \times M_{w(ALG)}, \quad (2)$$

where $M_{w(ALG)}$ is the molecular weight of the initial alginate taken from Table 1. Calculation according to equation 2 gives $M_{w(calc)} = 2.72 \times 10^3$ kDa for HG-1, 2.73×10^3 kDa for HG-2 and 2.74×10^3 kDa for HG-3. In other words, the molecular weight of the alginate hydrogels should practically not change if Ca^{2+} ions bind to the initial alginate macromolecules. However, in the experiment, a 16-fold increase in the molecular weight of the Ca^{2+} alginate hydrogel with $Z = 7$ is observed compared to the initial alginate (see Table 1).

The explanation for this observation is as follows. Binding of Ca^{2+} ions develops in two directions: as intrachain encapsulation of Ca^{2+} ions and as interchain ALG–ALG interaction through Ca^{2+} bridges. The latter becomes more noticeable with an increase in Ca^{2+} concentration in the reaction system. The data in Table 1 allows us to estimate the number of alginate macromolecules in the hydrogels: 2 in HG-1, 13 in HG-2 and 16 in HG-3.

At the same time, the hydrogel particle size decreases with increasing Ca^{2+} content. It looks like a paradox: the molecular weight of the hydrogel grows up, but its size goes down. To resolve the issue, let us turn to the composition of hydrogels or, more precisely, to the degree of cross-linking of hydrogels. This parameter is defined as the degree of participation of alginate carboxyl groups in interaction with Ca^{2+} ions, $\alpha \approx 2/Z_{Ca}$, and varies as 0.13 for HG-1, 0.2 for HG-2 and 0.29 for HG-3. It was observed that α changes more and more with increasing Ca^{2+} content and reaches a high value of 0.29 corresponding to a dense sphere. Comparing two factors, an increase in the molecular weight of the hydrogel and a rise in the degree of cross-linking, we conclude that it is the latter that determines the final size of the hydrogel particles.

It was reasonable to expect that residual carboxyl groups in Ca^{2+} alginate hydrogels could bind to cationic molecules. In accordance with this idea, the cationic fluorescent dye Rhodamine 6B (Rh) was incorporated into Ca^{2+} alginate hydrogels by mixing aqueous solutions of hydrogel and dye so that Z_{Rh} = [ALG]/[Rh] = 10 in each case. The resulting Ca^{2+}–alginate–rhodamine ternary hydrogel solutions were dialyzed against bidistilled water and lyophilized. The dried ternary hydrogels HG-1Rh, HG-2Rh and HG-3Rh were then dissolved in a Tris buffer solution (pH 7.2), and Rh was determined spectrophotometrically at 550 nm.[16] Over 99% of the initial Rh was found in ternary hydrogels.

An aqueous solution of the HG-1Rh hydrogel with a minimal Rh content was added to the medium of human colon adenocarcinoma HCT116 cells, and the kinetics of the Rh fluorescence in the cells was monitored using flow cytometry.[†] The results in Figure 1(*a*),(*b*) show an increase in cell fluorescence to a maximum during the first hour and negligible changes in fluorescence over the next 23 hours. In other words, the penetration of the Rh-containing hydrogel was completed within 1 hour after it was added to the cells.

The distribution of the penetrated Rh inside the cells was monitored using confocal microscopy after a 5-hour incubation of the hydrogel with the cells. As follows from the data in Figure 1(*b*), this time was sufficient for the maximum penetration of Rh. The microscopy experiment was performed under the same

[†] Flow cytometry measurements were performed using a BD Biosciences FACSCanto II instrument in the PE channel (excitation peak at 566 nm and emission peak at 574 nm). The data were analyzed using the FASCiva software.

Table 2 Cytotoxicity of hydrogels containing Dox and free Dox (control).[a]

Sample	IC_{50}/μM (Dox)		
	HCT116	MCF-7	Fibroblasts
Dox	0.56 ± 0.07	3.03 ± 0.2	0.55 ± 0.08
HG-1Dox	0.42 ± 0.04	3.01 ± 0.3	1.05 ± 0.2
HG-2Dox	0.43 ± 0.05	3.01 ± 0.3	1.34 ± 0.1
HG-3Dox	0.55 ± 0.06	3.02 ± 0.3	2.73 ± 0.2

[a] MTT assays were performed after 48 h of cell incubation with the specified sample.

conditions as the flow cytometry experiment described above. In Figure 1(*c*), there are three columns of images that reflect the fluorescence of HCT116 cells stained with the blue fluorescent dye Hoechst 33342 (left column), the Rh fluorescence (middle column) and the overlay of both fluorescent signals (right column). The conclusion that follows from these images is that Rh is diffusely distributed in the cytoplasm and does not penetrate into the cell nucleus.

Nuclear DNA is known to be a target for the antitumor antibiotic doxorubicin. Dox was incorporated into three Ca^{2+} alginate hydrogels with different Ca^{2+} contents by mixing aqueous solutions of HG-1, HG-2 and HG-3 hydrogels and an aqueous solution of Dox with Z_{Dox} = [ALG]/[Dox] = 10 in each case. The mixtures were dialyzed and lyophilized. Dried Ca^{2+}–alginate–Dox ternary hydrogels (HG-1Dox, HG-2Dox and HG-3Dox) were dissolved in a Tris buffer solution (pH 7.2) and analyzed spectrophotometrically at 574 nm. Over 99% of the initial Dox was found in the ternary hydrogels.

The biological activity of Dox in the ternary hydrogels was tested against three cell lines: HCT116 cells, human breast adenocarcinoma MCF-7 cells and hTERT-immortalized fibroblasts. The first and second lines are tumor cells, and the third is normal cells, but exhibiting the growth characteristics of a continuous cell line.[17] The cytotoxicity of the ternary hydrogels and free Dox (control) was assessed in *in vitro* experiments using a standard MTT assay[18] that quantifies the percentage of surviving cells. The half-maximal inhibitory concentration (IC_{50}) of Dox was taken as a measure of cytotoxicity (Table 2).

HCT116 cells showed higher sensitivity (lower IC_{50}) to Dox formulations compared to MCF-7 cells. Within each tumor cell line, a constancy of IC_{50} values was observed for both the initial Dox and the Dox incorporated in the hydrogels. Normal fibroblast cells showed a different behavior. For example, complexation with HG-3 resulted in a 5-fold decrease in Dox cytotoxicity. In general, Dox retained or even reduced its cytotoxicity after binding to the Ca^{2+} alginate hydrogels.

In summary, the cross-linking of anionic alginate with Ca^{2+} cations in an aqueous solution leads to Ca^{2+} alginate hydrogels, the particle size of which is in the range of 210–405 nm, depending on the amount of added Ca^{2+} salt. It was found that the resulting hydrogels can incorporate the cationic fluorescent dye Rhodamine or the cationic antitumor antibiotic doxorubicin. Rhodamine-containing hydrogels made it possible to reveal the maximum accumulation of the dye one hour after their addition to tumor cells. Doxorubicin incorporated into hydrogels retained or even reduced its toxicity to tumor and normal cells. The results obtained can be used in the development of containers for the encapsulation and delivery of drugs and the control of their interaction with cells.

This work was supported by the Russian Science Foundation (project no. 23-23-00156).

References

1 X. Meng, D. Yang, G. Keyvan, B. Michniak-Kohn and S. Mitra, *Colloids Surf., B*, 2012, **92**, 213.
2 J. Tamargo, J.-Y. Le Heuzey and P. Mabo, *Eur. J. Clin. Pharmacol.*, 2015, **71**, 549.
3 J. Herzberger, K. Niederer, H. Pohlit, J. Seiwert, M. Worm, F. R. Wurm and H. Frey, *Chem. Rev.*, 2016, **116**, 2170.
4 I. M. Higazy, A. A. Mahmoud, M. M. Ghorab and H. O. Ammar, *J. Drug Delivery Sci. Technol.*, 2021, **61**, 102274.
5 B. Tyler, D. Gullotti, A. Mangraviti, T. Utsuki and H. Brem, *Adv. Drug Delivery Rev.*, 2016, **107**, 163.
6 A. Angelova, V. M. Garamus, B. Angelov, Z. Tian, Y. Li and A. Zou, *Adv. Colloid Interface Sci.*, 2017, **249**, 331.
7 B. C. Evans, R. B. Fletcher, K. V. Kilchrist, E. A. Dailing, A. J. Mukalel, J. M. Colazo, M. Oliver, J. Cheung-Flynn, C. M. Brophy, J. W. Tierney, J. S. Isenberg, K. D. Hankenson, K. Ghimire, C. Lander, C. A. Gersbach and C. L. Duvall, *Nat. Commun.*, 2019, **10**, 5012.
8 M. Yu. Gorshkova, L. V. Vanchugova, I. F. Volkova, I. V. Obydennova, I. L. Valuev and L. I. Valuev, *Mendeleev Commun.*, 2022, **32**, 189.
9 E. V. Popova, P. V. Morozova, M. V. Uspenskaya and A. S. Radilov, *Russ. Chem. Bull.*, 2021, **70**, 1335.
10 L. W. Chan, Y. Jin and P. W. S. Heng, *Int. J. Pharm.*, 2002, **242**, 255.
11 T. Agarwal, S. N. G. H. Narayana, K. Pal, K. Pramanik, S. Giri and I. Banerjee, *Int. J. Biol. Macromol.*, 2015, **75**, 409.
12 Y. Sun, X. Jing, X. Ma, Y. Feng and H. Hu, *Int. J. Mol. Sci.*, 2020, **21**, 9159.
13 F. Esseku and M. C. Adeyeye, *Crit. Rev. Ther. Drug Carrier Syst.*, 2011, **28**, 395.
14 V. V. Spiridonov, K. S. Sadovnikov, D. A. Vasilenko, K. N. Sedenkova, A. R. Lukmanova, A. A. Markova, A. V. Shibaeva, A. V. Bolshakova, S. S. Karlov, E. B. Averina and A. A. Yaroslavov, *Mendeleev Commun.*, 2022, **32**, 591.
15 A. Zahoor, S. Sharma and G. K. Khuller, *Int. J. Antimicrob. Agents*, 2005, **26**, 298.
16 P. Bartasun, H. Cieśliński, A. Bujacz, A. Wierzbicka-Woś and J. Kur, *PLoS One*, 2013, **8**, e55697.
17 K. Yachi, H. Kikuchi, N. Suzuki, R. Atsumi, M. Aonuma and Y. Kawato, *Biopharm. Drug Dispos.*, 1995, **16**, 653.
18 X. Wang, Y. Xia, L. Liu, M. Liu, N. Gu, H. Guang and F. Zhang, *J. Biomed. Mater. Res., Part B*, 2010, **95**, 357.

Received: 31st January 2023; Com. 23/7093